Microbial Community Characteristics of Sediment Environment and Plastisphere in a Typical Highly Urbanized River Basin

Xingye Chen[1,#], Hongbo Su[1,#], Yuanhang Zhang[1] and Xin Qian[1,2,*]

[1]*School of Environment, State Key Laboratory of Water Pollution Control and Green Resource Recycling, Nanjing University, Nanjing, 210023, China*

[2]*Jiangsu Collaborative Innovation Center of Atmospheric Environment and Equipment Technology (CICAEET), Nanjing University of Information Science & Technology, Nanjing, 210044, China*

Abstract: Microplastics (MPs) provide surfaces for microbial colonization, yet field-based comparisons between plastisphere and surrounding sediment communities in urban rivers remain limited. We investigated sediments from a typical highly urbanized river basin—the Qinhuai River Basin, China—during normal flow (March 2025) and high flow (June 2025). We characterized MP abundance and particle features and compared bacterial and fungal communities in sediment and plastisphere samples using 16S rRNA V4 and ITS1 amplicon sequencing. MPs were detected in all valid samples, yielding 316 particles. Mean abundances were 178.35 ± 97.73 and 158.47 ± 143.18 particles kg^{-1} dry weight during normal and high flow, respectively; fragments and fibers dominated, and PET was the most frequent polymer among μ-FTIR-analyzed particles. Sediment communities had higher richness and diversity than plastisphere communities for both bacteria and fungi. Community composition differed between habitats (PERMANOVA: bacterial R^2 = 0.06888, p = 0.001; fungal R^2 = 0.04495, p = 0.002), although the proportion of variation explained by habitat was relatively small. Pseudomonadota and Ascomycota were relatively enriched in the plastisphere. CCA indicated that bacterial variation was associated with TN, NH_3-N, water content, and SOC, whereas fungal variation was associated with NH_3-N, water content, and TN. Mantel tests linked sediment bacterial community dissimilarity to between-sample differences in PET and PE variables, and fungal community dissimilarity to differences in PVC. These findings indicate modest habitat-associated differences in community composition, alongside associations with sediment properties and microplastic characteristics.

Keywords: 16S rRNA, Amplicon sequencing, Fungi, Microplastics, Plastisphere, Qinhuai River, Sediment.

1. INTRODUCTION

Plastic production and use have expanded rapidly because plastics are inexpensive, easily processed, and durable. Cumulative production reached approximately 8.3 billion tonnes by 2015, and annual production has exceeded 400 million tonnes in recent years, whereas recycling remains limited [1, 2]. Plastic waste enters the environment during production, use, transport, and disposal, and subsequently fragments through ultraviolet radiation, mechanical abrasion, and weathering [3-5]. Microplastics (MPs), commonly defined as particles smaller than 5 mm [6, 7], occur in aquatic, terrestrial, and atmospheric environments [3, 8, 9]. Rivers transport MPs from land to downstream waters [10, 11], whereas sediments retain these particles and serve as archives of longer-term contamination [12-14].

Urban rivers receive MPs through wastewater discharge, surface runoff, and the fragmentation of discarded plastic products [10, 15]. Sediment inventories reflect both external inputs and local retention [13, 14]. Particle abundance, size, color, and morphology provide complementary information for interpreting potential sources and microbial colonization, although visual traits alone cannot establish particle origin [10, 13].

MPs also provide surfaces for microbial colonization. Their hydrophobic interfaces can accumulate organic matter, nutrients, and co-occurring contaminants, creating localized microenvironments [16-18]. These attached microbial communities are collectively termed the plastisphere, and their composition may differ from that of surrounding microbial communities [16, 17, 19].

Comparing the plastisphere with surrounding sediment addresses habitat contrast within a particle-rich matrix. Sediment contains mineral particles, organic matter, and heterogeneous microsites that differ from a plastic surface. Therefore, results from plastic–water comparisons cannot be assumed to predict the direction or magnitude of plastic–sediment differences [17].

Previous studies have begun to examine these compartments, but their designs have addressed different parts of the problem. Niu *et al*. examined vertical variation in microplastic-associated bacterial communities and their relationships with surrounding sediment communities in an urban river [20]. Song *et al*. compared bacterial communities in eutrophic lake sediment and in the plastisphere using sediment microcosms, with emphasis on phosphorus-related

*Address correspondence to this author at the School of Environment, State Key Laboratory of Water Pollution Control and Green Resource Recycling, Nanjing University, Nanjing, 210023, China; E-mail: xqian@nju.edu.cn

#These authors contribute equally to this work

Received on 09-09-2026 Accepted on 21-10-2026 Published on 27-10-2026

E-ISSN: 2311-8741/26

processes [21]. Kettner *et al*. reported that fungal communities attached to polyethylene and polystyrene differed from fungal communities in surrounding water and on natural wood across several aquatic environments [22]. In addition, Nguyen *et al*. showed that bacterial plastisphere communities in urban-river water reactors were structured by organic content, salinity, and dissolved oxygen [23]. More recently, Chigwada *et al*. characterized bacterial and fungal communities associated with PE and PS debris in the urban Jukskei River [24]. These studies demonstrate the relevance of sediment context, plastic substrates, and environmental conditions to plastisphere communities. However, comparative evidence remains limited on whether bacterial and fungal assemblages exhibit concordant or contrasting plastisphere–sediment differences across flow periods in urban rivers.

Here, we addressed this gap by comparing bacterial and fungal communities in sediment and plastisphere samples collected from the same sites and sampling periods in the highly urbanized Qinhuai River Basin. Bacterial and fungal assemblages were analyzed separately using 16S rRNA V4 and ITS1 amplicon sequencing. We evaluated habitat-associated differences in taxonomic membership, dominant taxa, alpha diversity, and beta diversity, and examined associations with sediment properties and microplastic characteristics. The contribution of this study is therefore the parallel field assessment of bacterial and fungal habitat contrasts in urban-river sediments, rather than the assumption that bacterial patterns can represent fungal responses.

2. MATERIALS AND METHODS

2.1. Study Area and Sampling Design

The Qinhuai River Basin, a typical highly urbanized river basin in Nanjing, Jiangsu Province, China, was selected as the study area. The Qinhuai River lies in the lower reaches of the Yangtze River and is a major first-order tributary on its right bank. The basin covers approximately 2,631 km^2 and extends across the Qinhuai, Jiangning, and Lishui districts of Nanjing and Jurong City. Eleven sampling sites were established along the upper, middle, and lower reaches of the Qinhuai River, based on national and provincial monitoring sections and key river nodes. The locations of the 11 sites are shown in Figure **1**, and their names, river reaches, and geographic coordinates are listed in Supplementary Table **S3**.

Reach classification followed river connectivity rather than dividing the sites into equally sized groups. The upper reach encompasses the Jurong and Lishui tributaries upstream of their confluence near Xibei Village. The middle reach extends from that confluence toward Dongshuiguan, whereas the lower reach continues toward the Sanchahe outlet through the urban area. This classification provides geographic context for the grouped community profiles.

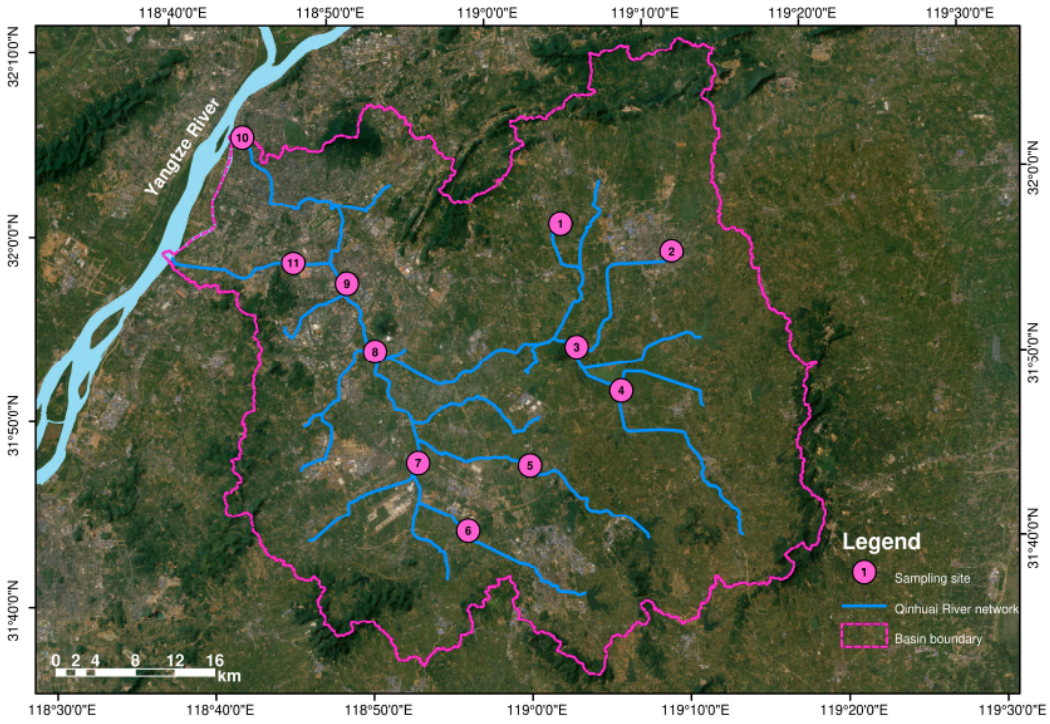


Figure 1: Study area and sampling sites in the Qinhuai River Basin, Nanjing, China. The map shows the basin boundary, river network, Yangtze River, and the 11 sampling sites. Sampling was conducted during the normal-flow (March 2025) and high-flow (June 2025) periods. Site numbers correspond to those in Supplementary Table S3, which lists site names and coordinates.

Sampling was conducted in March 2025 (normal flow) and June 2025 (high flow). Approximately 2,000 g of sediment was collected at each sampled site using a Peterson grab sampler. An approximately 2-g aliquot was transferred into a sterile 10-mL centrifuge tube using a sterilized stainless-steel spatula, transported under cooled conditions, and stored at −80°C for sediment microbial analysis. Separate portions of the remaining sediment were used for physicochemical measurements, microplastic characterization, and plastisphere sample preparation. Sediment and plastisphere samples therefore represented different analytical fractions of sediment collected at the same site and sampling occasion. Plastisphere samples consisted of biofilms recovered from selected plastic fragments, as described in Section 2.3.

The community datasets represented 10 sites in March (sites 1–10) and 11 sites in June (sites 1–11), corresponding to 21 site–sampling occasion combinations. No March samples from site 11 were included in either sequencing dataset. The bacterial dataset comprised 42 samples, with 10 sediment and 10 plastisphere samples from March and 11 sediment and 11 plastisphere samples from June. The fungal dataset comprised 39 samples, with 10 sediment and eight plastisphere samples from March and 11 sediment and 10 plastisphere samples from June. Usable ITS sequencing data were not obtained for three plastisphere samples (MP03_2, MP03_7, and MP06_9), although these samples were represented in the bacterial dataset. Samples collected in October 2024 belonged to a separate batch and were not included in the community analyses reported here.

2.2. Extraction and Identification of Sediment Microplastics

During the normal-flow period, ten sites yielded valid microscopy records; site 11 was excluded from the normal-flow abundance and composition statistics. Microscopy records and amplicon-sequencing sample counts were summarized separately.

Sediment samples were dried at 55°C, cooled to room temperature, and weighed on a dry-weight basis. For each sample, 100–150 g of sediment was mixed with 100 mL of $ZnCl_2$ solution adjusted to a density of approximately 1.65 g cm^{-3}. The suspension was sonicated for 30 min and allowed to stand for 1 h; the supernatant was then collected, and density separation was repeated three times. The remaining material was then treated with 20 mL of 0.05 mol L^{-1} $FeSO_4$ solution and 20 mL of 30% H_2O_2 and allowed to react for 96 h to digest natural organic matter [25, 26]. The digest was vacuum-filtered through a 20-μm nylon membrane, which was transferred to a clean glass Petri dish for microscopy and polymer analysis [27, 28]. The recovered particle counts therefore represent the operational fraction retained by this workflow.

Visual sorting based on particle morphology and color was used for preliminary screening of suspected microplastics [27]. The dried filters were systematically examined under a stereomicroscope (MZ62, Guangzhou Mingmei), and candidate particles were photographed and characterized by size, color, and morphology. In this study, particles were classified as suspected microplastics when they met at least two of the following visual criteria: absence of cellular structures, uniform coloration, a fibrous or other typical plastic morphology, homogeneous texture, and a glossy or glass-like appearance. This screening provided the particle inventory used to describe abundance and physical characteristics.

Selected particles were subsequently analyzed by μ-FTIR for chemical identification [28]. Approximately 10 suspected microplastic particles were randomly selected from each sample filter. Spectra were acquired using a Vertex 70v system (Bruker), with OPUS 5.0 acquisition software, at a spectral resolution of 2 cm^{-1} over 4,000–600 cm^{-1}, using 32 scans. The resulting spectra were compared with reference library spectra using OMNIC software. In this study, a library match of at least 70% was used as the acceptance criterion for polymer or resin assignments.

The final μ-FTIR composition dataset contained 147 records from 21 sediment samples, including 52 records from the normal-flow period and 95 from the high-flow period. Resin components were also included in the microplastic composition analysis with reference to ISO 24187:2023 [29]. Polymer and resin percentages were calculated using these 147 records as the denominator. The microscopy inventory comprised 316 visually identified suspected microplastic particles and was reported separately from the μ-FTIR dataset. Because only selected particles underwent spectroscopic analysis, the polymer assignments and percentages characterize the analyzed subset and were not extrapolated to the entire microscopy inventory.

2.3. Processing of Sediment and Plastisphere Samples

Sediment samples, representing the sediment environment, consisted of approximately 2 g of sediment collected in the field. They were transported to the laboratory under cooled conditions and stored at −80°C for subsequent DNA extraction and amplicon sequencing.

Plastisphere samples were processed after the material was returned to the laboratory. Larger microplastic fragments, approximately 1–5 mm in size, were picked with sterile forceps and placed in 10-mL sterile centrifuge tubes. Sterile phosphate-buffered saline (PBS) was added until the particles were fully submerged. The tubes were sonicated for 1 min and vortexed for 10 s; this cycle was repeated twice to transfer surface biofilm into the liquid phase. The eluate was filtered through a 0.22-μm hydrophilic membrane, retaining microorganisms on the membrane. The membrane was snap-frozen in liquid nitrogen and stored at −80°C for subsequent DNA extraction and amplicon sequencing.

2.4. Amplicon Sequencing of Bacterial and Fungal Communities

The V4 region of the 16S rRNA gene was amplified with primers 515F and 806R. Paired-end reads were quality-filtered with fastp [30]: terminal bases with a quality score below 20 were trimmed using a 50-bp sliding window, and reads shorter than 50 bp or containing more than five ambiguous bases (N) were removed. Paired reads were merged with FLASH using a minimum overlap of 10 bp and a maximum overlap mismatch ratio of 0.2. Barcode mismatches were not allowed, and up to two primer mismatches were permitted. Sequences were clustered with USEARCH at 97% identity, and chimeric sequences were removed. Taxonomic annotation was performed with RDPClassifier against the SILVA 138.2/16S database using a 70% confidence threshold, and chloroplast and mitochondrial sequences were removed according to the documented workflow. The 42 bacterial samples were rarefied to 43,098 sequences per sample, yielding 30,882 OTUs. Fungal communities were analyzed using the ITS1 region with primers ITS1F and ITS2R. The same quality-control, assembly, clustering, and chimera-removal workflow was applied, and taxonomy was assigned with RDPClassifier against the UNITE 9.0 ITS fungal database using a 70% confidence threshold. The 39 fungal samples were rarefied to 44,791 sequences per sample, yielding 7,454 fungal OTUs. The bacterial and fungal datasets were processed and analyzed separately using the available samples for each marker. Sample IDs and alpha diversity indices are provided in Supplementary Tables **S1** and **S2**, respectively.

The two marker datasets were evaluated separately throughout the community comparisons. OTU counts refer to operational taxonomic units defined within each dataset, rather than direct counts of microbial cells. The use of different marker regions also means that bacterial and fungal OTU totals are not equivalent measures of organism abundance. Within each dataset, taxonomic membership and relative abundance provide complementary descriptions of the recovered community. The present comparisons therefore describe marker-defined bacterial and fungal assemblages in the sediment environment and plastisphere.

2.5. Measurement of Sediment Physicochemical Properties

Sediment environmental variables included ammonia nitrogen (NH_3-N), total nitrogen (TN), total phosphorus (TP), sediment organic carbon (SOC), and water content (H_2O). NH_3-N was measured in fresh samples: approximately 40 g of sediment was collected in the field, stored at 4°C, and analyzed within 3 days. TN, TP, and SOC were measured in air-dried samples. After natural air-drying, samples were ground using a ball mill, passed through a 100-mesh stainless-steel sieve (approximately 0.149 mm aperture), and approximately 3 g was weighed for each determination. Water content was calculated from the wet mass and oven-dried mass of the sediment [31].

The physicochemical protocol involved potassium chloride extraction and spectrophotometric determination of inorganic nitrogen following HJ 634-2012. Measurements were performed using a UV-visible spectrophotometer. The reference methods for TN, TP, and SOC were LY/T 1228-2015, LY/T 1232-2015, and NY/T 1141.6-2006, respectively. These measurements characterize the sediment matrix associated with the community samples.

2.6. Quality Control

Direct contact between samples and potential plastic contamination sources was avoided during sampling and laboratory processing. Personnel wore natural latex gloves and cotton laboratory coats and worked in a clean bench; laboratory doors and windows were kept closed, and sample exposure time was minimized. Glassware was used throughout, and all open containers were covered with aluminum foil. The high-purity water used for washing glassware and preparing solutions was prefiltered through a 0.45-μm glass-fiber membrane. Blank controls consisted of 100 mL of filtered pure water subjected to the complete sediment-sample procedure. A single microplastic particle was recorded across the three blanks, and the background level was considered negligible.

2.7. Data Analysis and Statistics

MP abundance was calculated on a dry-weight basis and expressed as particles kg^{-1} (dw). Data were organized in Microsoft Excel, and statistical analysis and visualization were performed using R 4.1.3 and

Origin. Alpha and beta diversity calculations were performed using Mothur [32], and bacterial and fungal datasets were analyzed separately. Unless otherwise stated, $p < 0.05$ was considered statistically significant.

Alpha diversity indices included Sobs, Chao1, ACE, Shannon, and Simpson. Beta diversity was based on Bray-Curtis distances. Principal coordinates analysis (PCoA) and nonmetric multidimensional scaling (NMDS) were used to visualize habitat-associated patterns, and permutational multivariate analysis of variance (PERMANOVA) was used to test differences in community composition. Wilcoxon rank-sum tests were used for habitat comparisons of diversity indices and taxonomic units. Differential taxa were identified using linear discriminant analysis effect size (LEfSe) [33], with an LDA score threshold greater than 4.

False discovery rate (FDR) correction was applied to alpha diversity comparisons, and Bonferroni correction was applied to phylum-level comparisons.

For particle descriptions, the study defined five size classes: below 100, 100–200, 200–500, 500–1,000, and above 1,000 μm. Size, color, and morphology were summarized as count-based composition variables. The pooled composition describes the combined particle inventory, whereas site-specific profiles preserve variation among sampling locations. These summaries differ: pooling particles gives greater weight to samples containing more counted particles. Accordingly, pooled percentages were not interpreted as equally weighted averages of site-level proportions. The flow-period-specific denominators followed the valid microscopy records, with the missing normal-flow record retained as missing.

Associations between community composition and sediment environmental factors were evaluated using Spearman correlation analysis and canonical correspondence analysis (CCA). Detrended correspondence analysis (DCA) was performed before environmental-factor ordination; when the gradient length reached or exceeded 3.5, CCA was used to evaluate genus-level bacterial and fungal community composition in relation to TN, TP, NH_3-N, SOC, and H_2O. Mantel tests were conducted at the genus level using Bray-Curtis distances for community composition and Euclidean distances for environmental-factor and MP characteristic matrices; Spearman correlation was used to evaluate relationships among the measured variables.

3. RESULTS

3.1. Microplastic Characteristics

Across the normal-flow period in March 2025 and the high-flow period in June 2025, 21 valid microscopic records were obtained, representing 10 and 11 sites, respectively. MPs were detected in all valid records. Mean MP abundances were 178.35 ± 97.73 and 158.47 ± 143.18 particles kg^{-1} dry weight during normal and high flow, respectively, with ranges of 40.53–355.73 and 45.53–467.68 particles kg^{-1} dry weight. Of the 10 sites with valid records in both periods, MP abundance was higher during high flow at four sites and during normal flow at the other six (Figure **2**). Site 11 lacked a valid microscopy record during the normal-flow period and was therefore excluded from the statistics for that period.

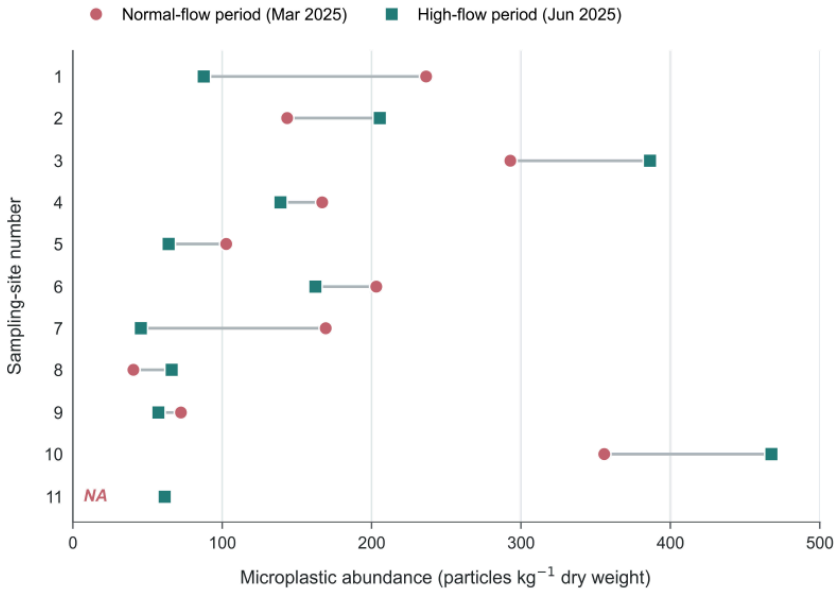


Figure 2: Microplastic abundance at the 11 sampling sites during the normal-flow (March 2025) and high-flow (June 2025) periods, expressed as particles kg^{-1} dry weight. Connecting lines link observations from the same site. NA indicates an unavailable observation.

Visual screening yielded 316 suspected microplastic particles across the two periods, including 163 during the normal-flow period and 153 during the high-flow period. After pooling particle counts, the 200–500 μm size class was the most abundant (34.8%). Fragments and fibers dominated the morphology, accounting for 52.5% and 38.9%, respectively. Green and red were the most common colors, accounting for 24.1% and 20.9%, respectively. Fragments and fibers dominated in both periods; red particles were most common during normal flow, whereas green particles were most common during high flow. These percentages are count-based proportions for the corresponding particle set; site- and flow-period-specific compositions are shown in Figure **3**. Polymer analysis included 147 records for selected particles (52 normal-flow and 95 high-flow), providing the polymer-composition profile of the analyzed subset.

Among the 147 selected μ-FTIR records, PET was the most frequent assignment (30 records, 20.41%), followed by PE (21, 14.29%), epoxy resin (18, 12.24%), PP (18, 12.24%), PVC (9, 6.12%), PVDF (8, 5.44%), and PVAL (5, 3.40%). Less frequent polymer and resin assignments are listed in Table **1**. These percentages describe the selected spectral subset and were not extrapolated to all 316 particles recorded by microscopy.

Representative candidate particles observed during stereomicroscopic screening are shown in Figure **4**.

3.2. Bacterial and Fungal Community Composition

The normal-flow sediment, normal-flow plastisphere, high-flow sediment, and high-flow plastisphere samples were treated as four groups. The four groups shared 7,067 16S OTUs, representing 22.88% of the union of the four sets. The normal-flow and high-flow plastisphere groups contained 2,681 and 2,805 16S OTUs detected only in the respective groups, whereas the corresponding sediment groups contained 2,308 and 3,807. The four fungal groups shared 287 OTUs,

Table 1: Polymer and resin assignments in the selected μ-FTIR dataset. Counts (*n*) and percentages are based on 147 records, comprising 52 from the normal-flow period and 95 from the high-flow period

Assignment	Abbreviation	n	Percentage (%)
Polyethylene terephthalate	PET	30	20.41
Polyethylene	PE	21	14.29
Epoxy resin	—	18	12.24
Polypropylene	PP	18	12.24
Poly(vinyl chloride)	PVC	9	6.12
Poly(vinylidene fluoride)	PVDF	8	5.44
Poly(vinyl alcohol)	PVAL	5	3.40
Phenol resin	—	4	2.72
Phenoxy resin	—	4	2.72
Polystyrene	PS	4	2.72
Polytetrafluoroethylene	PTFE	3	2.04
Polycarbonate	PC	3	2.04
Polyepichlorohydrin	PECH	2	1.36
Furan resin	—	2	1.36
Polyacrylonitrile	PAN	2	1.36
Polyoctamethylene	—	2	1.36
Poly(vinylidene chloride)	PVDC	2	1.36
Polybutylene sulfone	PBSF	2	1.36
Polyamide	PA	2	1.36
Polyalkene	—	2	1.36
Poly(vinyl butyral)	PVB	1	0.68
Polydiallylisophthalate	—	1	0.68
Polymethylcaprolactam	—	1	0.68
Poly(vinyl acetate)	PVAc	1	0.68

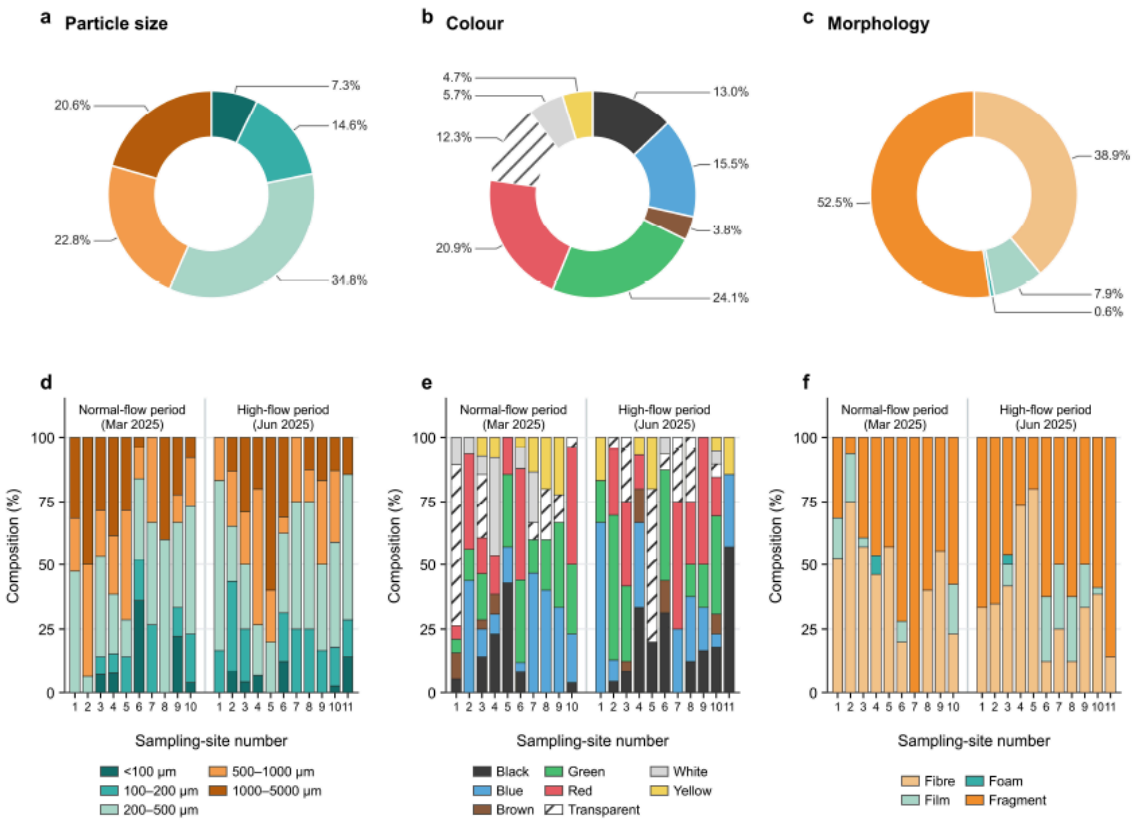


Figure 3: Size, color, and morphology of recovered microplastics. (**a**–**c**) Pooled particle-count compositions for size, color, and morphology, respectively; (**d**–**f**) corresponding compositions by sampling site and flow period. Percentages were calculated from all 316 particles in (**a**–**c**) and from the particles at each site within each flow period in (**d**–**f**). The dataset includes 10 sites in the normal-flow period and 11 sites in the high-flow period. Sampling-site numbers correspond to those shown in Figure 1 and listed in Supplementary Table S3.

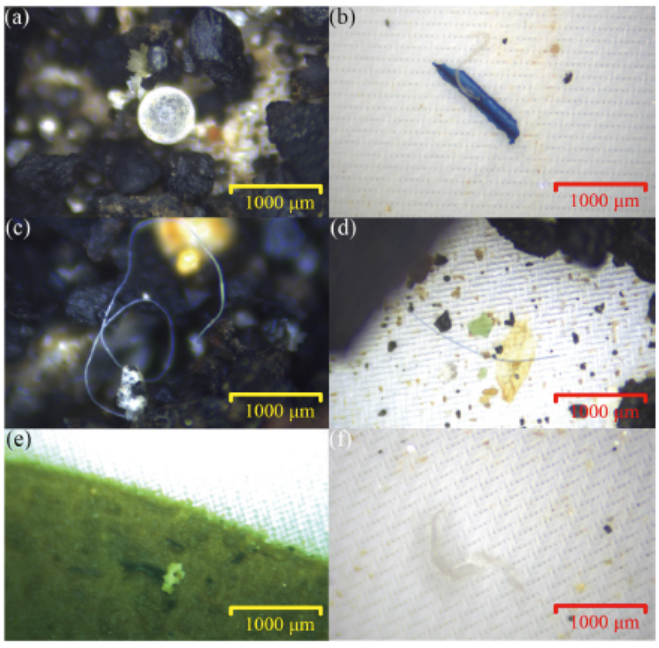


Figure 4: Representative candidate particles observed during stereomicroscopic screening: (**a**) spherical particle; (**b**) fragment; (**c**) fiber; (**d**) fragment and fiber; (**e**) foam; and (**f**) film. Scale bars: 1000 µm.

representing 3.85% of the union of the four fungal sets. The normal-flow and high-flow sediment groups contained 2,601 and 1,464 group-specific fungal OTUs, respectively, whereas the corresponding plastisphere groups contained 309 and 313. Thus, in both flow-period groupings, the sediment environment had more group-specific fungal OTUs than the corresponding plastisphere habitat (Figure **5**).

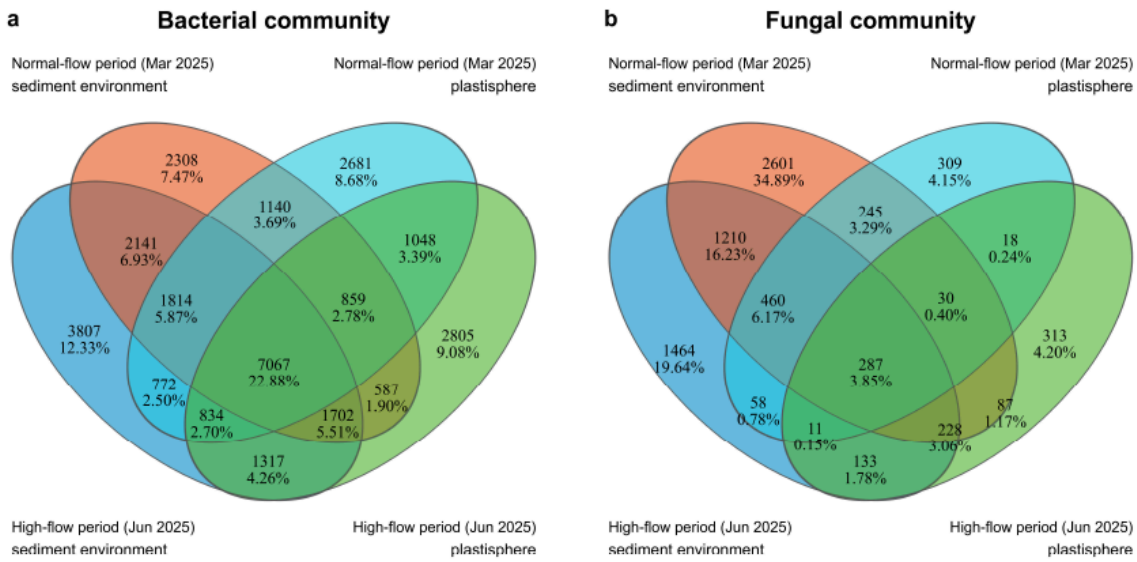


Figure 5: Overlap of operational taxonomic units (OTUs) among habitats and flow periods. (**a**) Bacterial communities; (**b**) Fungal communities. The four groups represent sediment and plastisphere samples from the normal-flow and high-flow periods. Numbers indicate OTU counts, and percentages were calculated relative to the union of the four OTU sets within each marker dataset.

The four-group 16S and fungal sets showed different membership patterns across the two sampling periods. In the 16S dataset, group-specific OTUs were more numerous in the plastisphere during normal flow but in the sediment environment during high flow. For fungi, the sediment groups contained more group-specific OTUs in both periods. Thus, the direction of the 16S membership contrast changed between campaigns, whereas the fungal contrast retained the same direction. This comparison describes detected group membership only; it does not determine whether an OTU absent from one set was biologically absent or remained below the detection threshold.

When samples from both flow periods were pooled, Pseudomonadota accounted for 27.47% of the bacterial community in sediment and 34.43% in the plastisphere (Figure **6a**). For fungi, Ascomycota accounted for 20.81% in sediment and 38.98% in the plastisphere. Chytridiomycota had a higher relative abundance in sediment, whereas Basidiomycota had a higher relative abundance in the plastisphere (Figure **6c**).

The bacterial profiles also differed between flow periods (Figure **6b**). Pseudomonadota had a higher relative abundance in the plastisphere than in sediment during both periods. Within sediment, its relative abundance was higher during high flow than during normal flow, whereas the plastisphere showed the opposite pattern. Chloroflexota and Thermodesulfobacteriota had higher relative abundances during normal flow in both habitats.

For fungi, Ascomycota had a higher relative abundance in the plastisphere than in sediment during both periods (Figure **6d**). Within each habitat, Ascomycota had a higher relative abundance during high flow, whereas Chytridiomycota had a higher relative abundance during normal flow. Basidiomycota showed contrasting patterns between habitats, with a higher relative abundance during high flow in sediment but during normal flow in the plastisphere. These flow-period comparisons describe the relative-abundance profiles and do not establish statistically significant differences between periods.

3.3. Community Diversity and Differential Taxa

With samples from both flow periods pooled, bacterial richness and Shannon diversity were higher in sediment than in the plastisphere (Figure **7a**–**c**). Median Sobs, Chao1, and Shannon values were 5,009, 7,005.28, and 6.99 in sediment, compared with 3,735, 4,717.60, and 6.65 in the plastisphere, respectively. Wilcoxon rank-sum tests with FDR correction indicated significant habitat differences for Sobs ($p \leq 0.05$), Chao1 ($p \leq 0.01$), and Shannon ($p \leq 0.05$), based on 21 samples per habitat.

Fungal richness and Shannon diversity were also higher in sediment than in the plastisphere (Figure **7d**–**f**). Median Sobs, Chao1, and Shannon values were 767, 791.02, and 4.77 in sediment, compared with 154.5, 156.44, and 3.29 in the plastisphere, respectively. All three habitat comparisons were significant after FDR correction ($p \leq 0.001$), based on 21 sediment and 18 plastisphere samples.

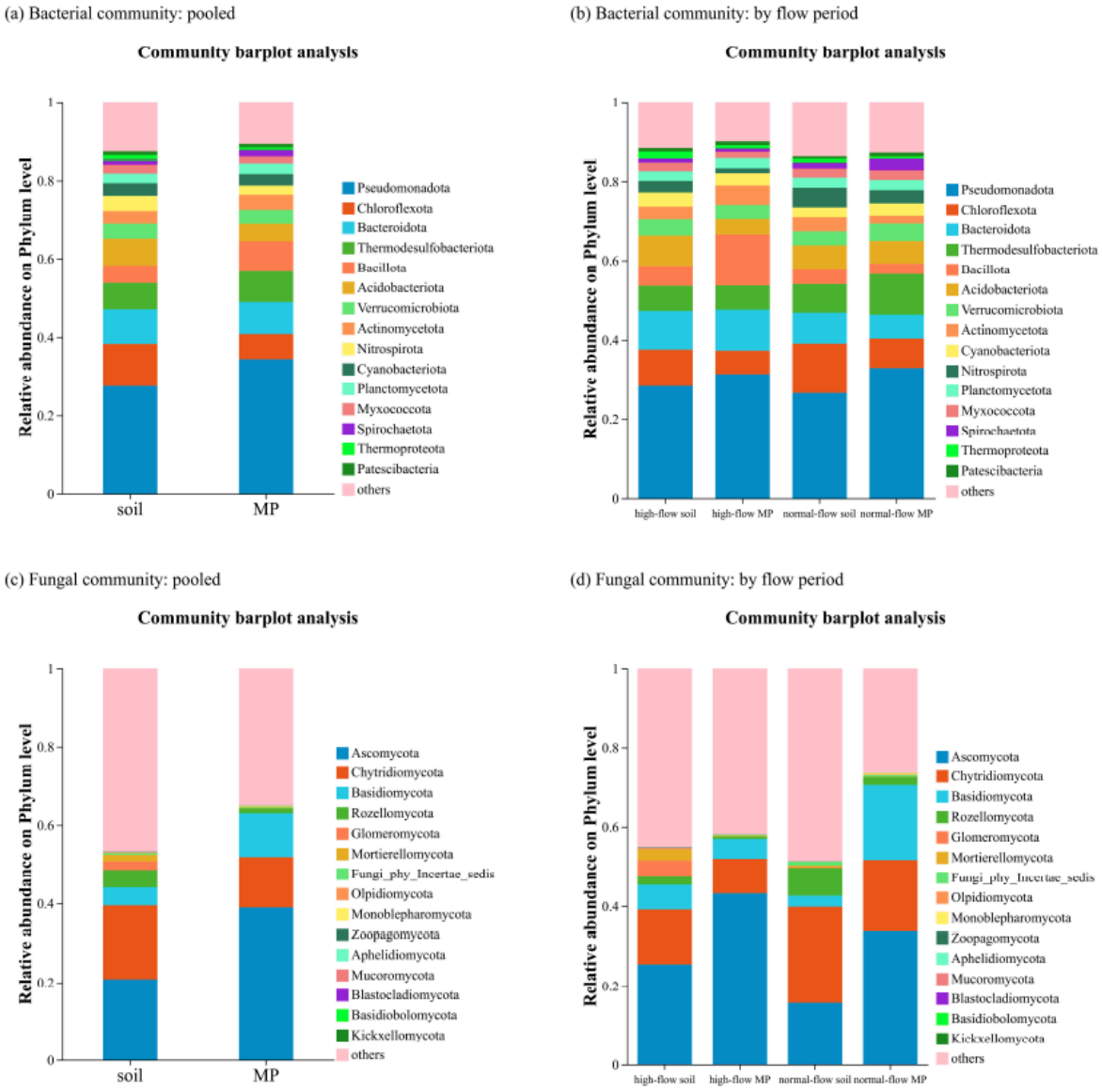


Figure 6: Phylum-level relative abundance of bacterial and fungal communities in the sediment environment and plastisphere. (**a**) Bacterial community, pooled across flow periods; (**b**) bacterial community by flow period; (**c**) fungal community, pooled across flow periods; (**d**) fungal community by flow period. Relative abundance is shown at the phylum level. Taxa not shown individually are grouped as "others". Soil, sediment environment; MP, plastisphere; normal-flow, normal-flow period (March 2025); high-flow, high-flow period (June 2025).

Descriptive summaries by flow period showed higher median Sobs, Chao1, and Shannon values in sediment than in the plastisphere for both microbial groups during both periods (Supplementary Tables **S1** and **S2**). Within each habitat, median Sobs and Chao1 values were lower in June than in March for both bacteria and fungi. Median fungal Shannon values were also lower in June, whereas bacterial Shannon values were similar or higher. These period-specific summaries are descriptive; the significance tests reported above concern habitat differences with both periods pooled.

Rarefaction curves provide context for the richness comparisons (Supplementary Figures **S1** and **S2**). Fungal Sobs curves approached a plateau, whereas 16S Sobs curves continued to rise with increasing sequence counts. The accompanying 16S Shannon curves flattened earlier, indicating that richness and diversity did not show identical responses to sequencing depth. These observations support reporting richness and diversity metrics separately.

With samples from both flow periods pooled, Bray–Curtis-based PCoA showed partial separation between sediment and plastisphere communities (Figure **8**). For bacteria, the first two axes explained 15.38% and 8.09% of the variation, respectively, and PERMANOVA detected a habitat difference (R^2 = 0.06888, p = 0.001). For fungi, the first two axes explained 9.14% and 4.99%, respectively, and the habitat difference was also significant (R^2 = 0.04495, p = 0.002). Habitat accounted for approximately 6.9% of bacterial and 4.5% of fungal community variation,

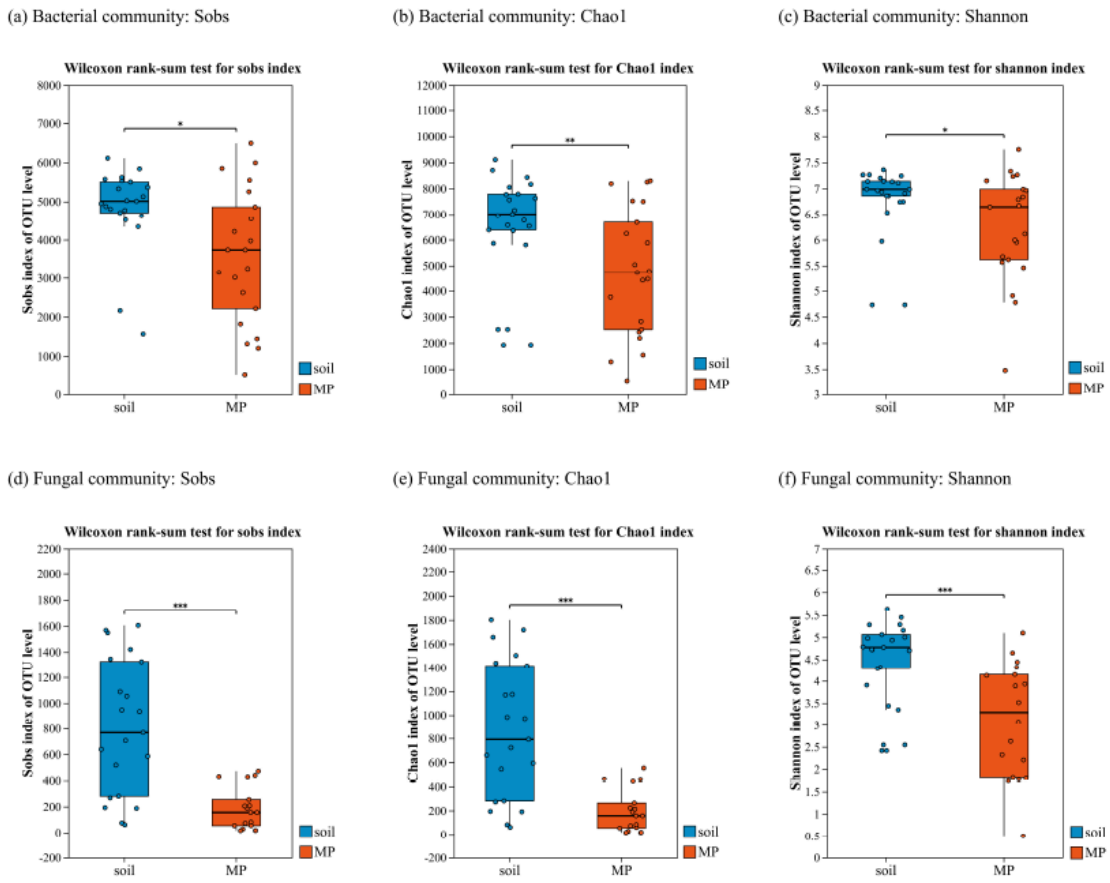


Figure 7: Alpha diversity of bacterial and fungal communities in the sediment environment and plastisphere. (**a**–**c**) Sobs, Chao1, and Shannon indices for bacterial communities, respectively; (**d**–**f**) corresponding fungal indices. Sample sizes were 21 sediment and 21 plastisphere samples for the 16S dataset and 21 sediment and 18 plastisphere samples for the fungal dataset. Points represent individual samples. Habitat differences were assessed with samples from both flow periods pooled, using Wilcoxon rank-sum tests with FDR correction: * $p \leq 0.05$; ** $p \leq 0.01$; *** $p \leq 0.001$. soil, sediment environment; MP, plastisphere.

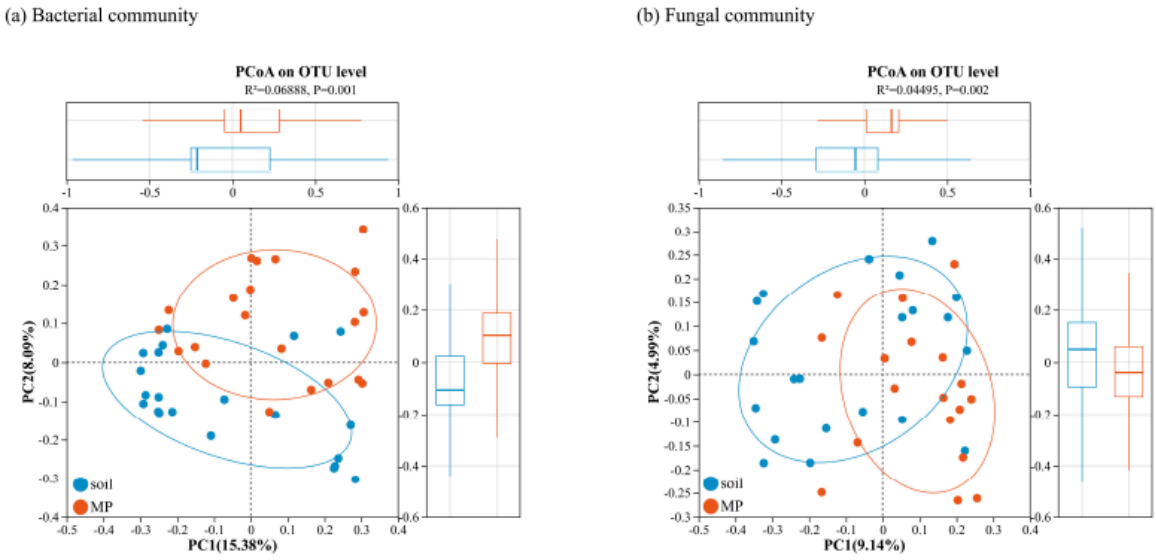


Figure 8: Principal coordinates analysis (PCoA) based on Bray–Curtis dissimilarity of (**a**) bacterial and (**b**) fungal communities. Points represent samples, and marginal boxplots summarize their scores along each axis. Axis percentages indicate the variation explained. R^2 and p values are from permutational multivariate analysis of variance (PERMANOVA). soil, sediment environment; MP, plastisphere.

indicating significant but modest differentiation between habitats.

NMDS provided a complementary ordination view (Supplementary Figure **S4**), with stress values of 0.15 for the 16S dataset and 0.192 for the fungal dataset.

The two habitats showed partially different distributions in ordination space; NMDS was interpreted as a complementary visualization rather than an independent test.

Wilcoxon rank-sum tests with Bonferroni correction showed that Ignavibacteriota was significantly enriched in the plastisphere ($p < 0.01$), whereas the other phyla shown in Supplementary Figure **S3a** were significantly more abundant in the sediment environment. Among

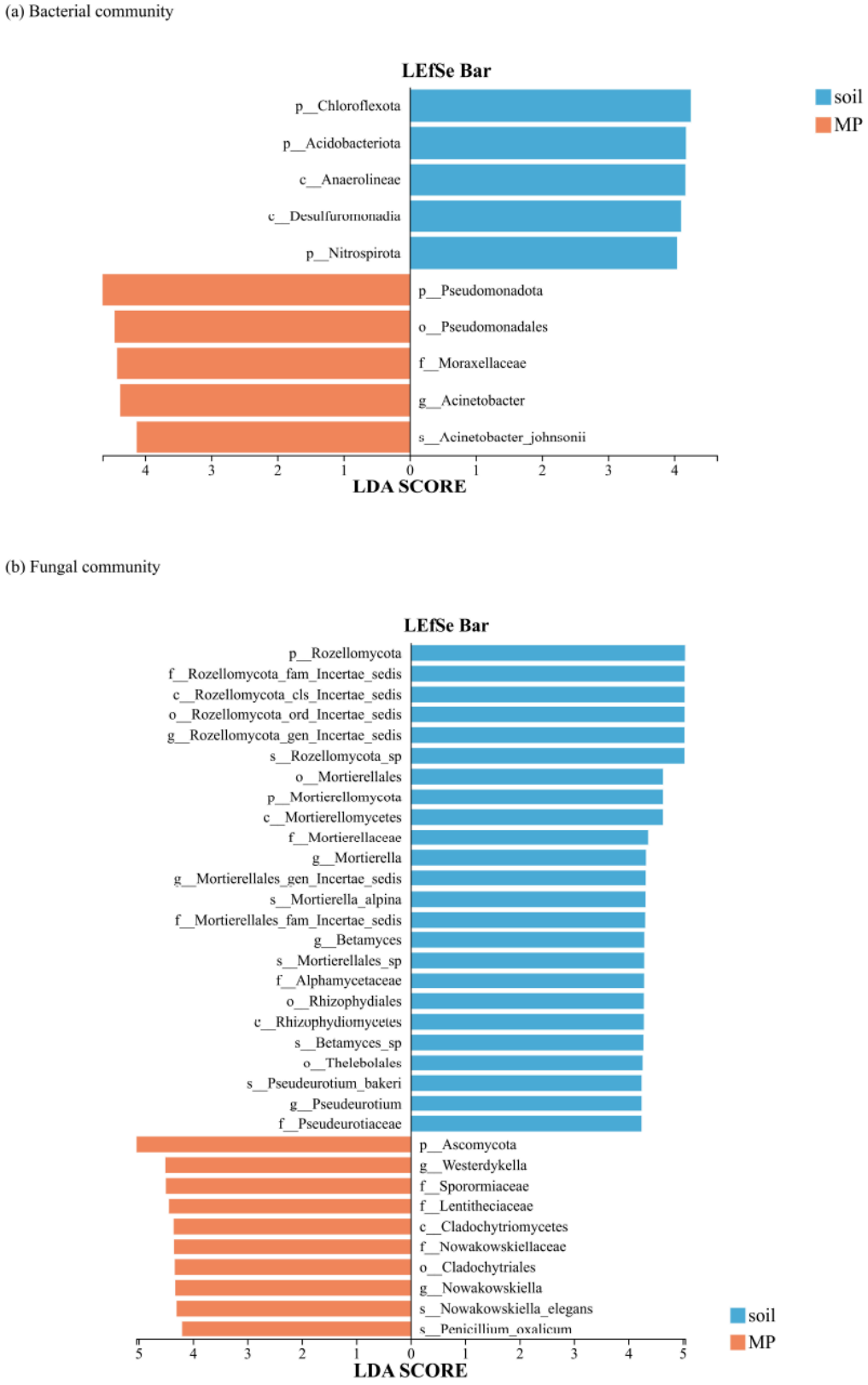


Figure 9: Linear discriminant analysis effect size (LEfSe) analysis of taxa differing between sediment environment and the plastisphere. (**a**) 16S-detected taxa; (**b**) Fungal taxa. Bars show LDA scores, with colors indicating the associated habitat. Taxonomic prefixes: p, phylum; c, class; o, order; f, family; g, genus; s, species. soil, sediment environment; MP, plastisphere.

fungi, Rozellomycota, Mortierellomycota, and Zoopagomycota had significantly higher relative abundances in sediment than in the plastisphere (Bonferroni-adjusted $p < 0.05$; Supplementary Figure **S3b**). These results identify taxa associated with the two habitat groups under the reported comparisons.

LEfSe identified habitat-associated 16S-detected phyla and taxa, together with habitat-associated fungal taxa, at multiple taxonomic levels (Figure **9**). Chloroflexota, Acidobacteriota, and Nitrospirota were associated with the sediment environment, whereas Pseudomonadota and Acinetobacter were associated with the plastisphere. Rozellomycota and Mortierellomycota were associated with the sediment environment, whereas Ascomycota, *Westerdykella*, and *Nowakowskiella* were associated with the plastisphere. These marker taxa describe multilevel differences between the two habitats.

3.4. Relationships between Environmental Factors and Microbial Community Composition

CCA related genus-level bacterial and fungal community composition to TN, TP, NH_3-N, SOC, and H_2O (Figure **10**). In the bacterial ordination, the TN, NH_3-N, H_2O, and SOC vectors pointed toward negative CCA1 scores, whereas TP was oriented mainly toward negative CCA2 scores. In the fungal ordination, NH_3-N, H_2O, and TN vectors extended toward negative CCA1 scores, while the TP vector extended toward negative scores on both axes; some plastisphere samples were positioned in the direction of the TP vector. These patterns indicate associations between sediment nutrients, water content, and community distributions, with the relative patterns differing between the two marker datasets.

For sediment communities, Mantel tests showed positive correlations between bacterial community dissimilarity and between-sample differences in the PET and PE variables, and between fungal community dissimilarity and differences in the PVC variable ($p < 0.05$; Supplementary Figure **S5**). Thus, sample pairs that differed more in these polymer variables tended to have more dissimilar community compositions.

4. DISCUSSION

4.1. The Plastisphere Shows Habitat-Associated Community Differences from Surrounding Sediments

The plastisphere shared dominant phyla with surrounding sediment but differed in OTU membership, relative abundance, alpha diversity, and beta-diversity structure. Although the PERMANOVA results were statistically significant, habitat accounted for only approximately 6.9% of bacterial and 4.5% of fungal community variation. These results indicate modest habitat-associated differentiation and do not establish habitat as the dominant determinant of community structure or demonstrate functional consequences.

Sediment heterogeneity may support a broader range of niches, whereas plastic provides a more selective attachment surface on which biofilms develop [17]. Environmental conditions and polymer context can also influence plastisphere community composition [23, 34]. In an urban river, McCormick *et al*. also reported lower bacterial diversity on microplastics than in the water column and on suspended organic matter [35]. The lower diversity observed here should therefore be interpreted as a condition-specific habitat

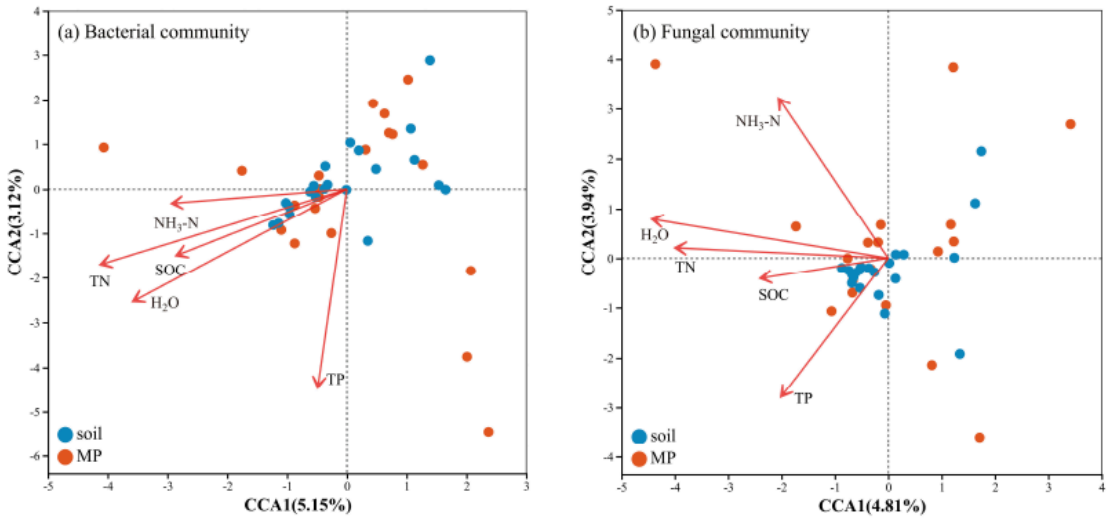


Figure 10: Canonical correspondence analysis (CCA) of genus-level (**a**) bacterial and (**b**) fungal communities in relation to sediment environmental variables. Points represent samples, and arrows indicate environmental gradients. TN, total nitrogen; TP, total phosphorus; NH_3-N, ammonia nitrogen; SOC, organic carbon; H_2O, water content. soil, sediment environment; MP, plastisphere.

contrast rather than a universal property of plastisphere communities.

4.2. Bacterial and Fungal Responses Differ among Taxa

Although sediment communities had higher alpha diversity in both marker datasets, bacterial and fungal taxonomic patterns were not fully concordant. This indicates that habitat-associated differences were taxon-specific rather than uniform across the two microbial groups.

Across nine European river-to-sea systems, fungal communities differed between microplastics and surrounding waters, and their composition varied along the freshwater–marine gradient [36]. Ascomycota had a higher relative abundance in the plastisphere, whereas Chytridiomycota had a higher relative abundance in sediment (Figure **6c**). These patterns identify candidate habitat-associated taxa, but, given the modest PERMANOVA effect sizes described in Section 4.1, they do not establish greater fungal sensitivity, substrate selection, or a single underlying mechanism.

4.3. Hydrological and Spatial Context Were Associated with Community Structure

Dominant taxa showed different responses across flow periods and habitats, indicating that hydrological change did not act uniformly across the community. Such shifts are consistent with habitat-dependent responses to changing river conditions [23, 34].

River position can modify transport, resuspension, organic-matter inputs, and particle retention, thereby changing exposure conditions for sediment and plastic surfaces [10, 11, 23]. For example, Hurley *et al*. documented substantial removal of microplastics from riverbed sediments following catchment-wide flooding [37]. This provides a plausible context for reach-specific community patterns and polymer associations.

4.4. Environmental Factors and Polymer Composition Are Associated with Community Differentiation

The CCA plots place the observed community differences in the context of sediment nutrient and organic carbon gradients (Figure **10**). In the bacterial ordination, TN, SOC, and water content vectors pointed in similar directions, suggesting that their relationships with community composition overlapped within the displayed ordination space. In the fungal ordination, NH_3-N and TP vectors pointed in different directions, indicating that the displayed nitrogen and phosphorus gradients were not interchangeable. Ecologically, these patterns are compatible with community variation across differing resource conditions. Freshwater biofilm research has likewise linked carbon-use profiles to nutrient conditions, including TN and TP [38]. However, TN, TP, and SOC measure bulk pools rather than directly available resources, so these patterns do not establish which nutrient, if any, limited microbial growth.

Experimental studies provide a basis for considering links between sediment community composition and nutrient cycling. In salt-marsh sediment microcosms, microplastic amendments altered microbial community composition and nitrogen cycling, with different responses among polymer treatments [39]. In eutrophic lake sediment microcosms, bacterial changes in the sediment and plastisphere were accompanied by changes in phosphorus availability following PET and PLA amendments [21]. These findings identify plausible connections among plastic substrates, microbial communities, and nutrient transformations. However, the present field survey measured community composition and sediment properties rather than nitrogen or phosphorus transformation rates. Its CCA and Mantel associations therefore cannot demonstrate the functional processes observed in those experiments.

Water content was measured in bulk sediment and may not represent conditions within plastic biofilms. Because sediment properties can covary with sampling location and flow period, the ordination patterns do not isolate independent environmental effects.

The associations of sediment bacterial communities with PET/PE and fungal communities with PVC may reflect several processes (Supplementary Figure **S5**). One possible ecological interpretation is that the measured polymer variables mark differences in plastic inputs and associated sediment conditions across samples. Plastic-related effects on communities are also plausible in light of the experimental studies discussed above, but the present survey cannot distinguish such effects from shared environmental variation. The different significance patterns do not establish bacterial preference for PET/PE or fungal preference for PVC, nor do they constitute a direct statistical comparison of bacterial and fungal responses. Interpretation is further limited by polymer characterization of only a selected particle subset and the absence of microbial sequencing resolved by polymer type (Section 4.5). Niu *et al*. investigated PE/PP biodegradation using long-term incubation and enrichment experiments combined with polymer characterization [40]. The present amplicon and correlation data provide no direct evidence of polymer

utilization or degradation. These findings therefore identify candidate polymer–community relationships for testing through polymer-specific sampling and controlled experiments.

4.5. Scope of the Community Analysis

The particle characterization has two limitations. First, visual identification cannot establish the polymer identity of every counted particle, so misclassification of particles without spectroscopic confirmation cannot be excluded. Second, μ-FTIR analysis covered only a selected subset, which may underrepresent uncommon polymers and may not reproduce the size, shape, or color distribution of the full particle inventory. The pooled polymer percentages also reflect unequal numbers of analyzed particles among samples and flow periods. They therefore describe the analyzed subset rather than an unbiased estimate of overall polymer composition. In addition, microbial sequencing targeted biofilms from a separate fraction of selected millimeter-scale fragments. Consequently, polymer–community associations cannot be interpreted as direct measurements of microbial colonization on individual spectroscopically identified particles.

5. CONCLUSIONS

Microplastics occurred in Qinhuai River sediments during both sampled flow periods, with fragments and fibers dominating the microscopy inventory and PET being the most frequently identified polymer in the μ-FTIR subset. For both bacteria and fungi, sediment communities had higher richness and Shannon diversity than plastisphere communities. Pseudomonadota and Ascomycota had higher relative abundances in the plastisphere. However, habitat accounted for only approximately 6.9% of bacterial and 4.5% of fungal community variation, indicating statistically significant but modest compositional differentiation. Community composition was also associated with sediment physicochemical gradients. In sediment samples, Mantel tests linked bacterial community dissimilarity to between-sample differences in PET and PE variables, and fungal community dissimilarity to differences in PVC.

For environmental monitoring of microplastic pollution in urban river sediments, these findings support combining particle abundance and representative spectroscopic characterization with sediment physicochemical measurements across sites and flow periods. Paired bacterial and fungal profiling of sediment and plastisphere communities could provide complementary ecological context. However, the use of these community patterns as indicators of microplastic-specific impacts requires independent validation.

The observational design and coverage of only two sampling occasions limit causal inference and temporal generalization. Polymer characterization relied on a selected particle subset, while plastisphere sequencing targeted separately selected fragments without resolving communities by polymer type. The observed associations therefore do not establish polymer-specific colonization, plastic degradation, or ecological harm. Repeated sampling and controlled studies combining polymer identification with microbial functional measurements would help assess the relevance of these associations for monitoring.

CONFLICT OF INTEREST STATEMENT

The Authors declare that there are no relevant financial or non-financial competing interests to report.

AUTHORS' CONTRIBUTION

Xingye Chen: Writing – original draft, Data curation. Hongbo Su: Conceptualization, investigation, Data curation. Yuanhang Zhang: Writing – review & editing. Xin Qian: Writing – review & editing, Funding acquisition.

FUNDING STATEMENT

This study was supported by National Natural Science Foundation of China (42577430).

SUPPLEMENTARY INFORMATION

Supplementary Figures **S1**–**S5** and Tables **S1**–**S3** are provided in the accompanying submission package. Supplementary Figures **S1**–**S2** show rarefaction curves, Supplementary Figure **S3** shows differential taxa, and Supplementary Figure **S4** shows NMDS ordinations. Supplementary Figure **S5** shows the Mantel networks. Supplementary Table **S3** provides the sampling-site information.

DATA AVAILABILITY

Data will be made available on request.

REFERENCES

[1] Geyer R, Jambeck JR, Law KL. Production, use, and fate of all plastics ever made. Science Advances 2017; 3(7): e1700782. https://doi.org/10.1126/sciadv.1700782

[2] Plastics Europe. Plastics – the fast Facts 2023. Plastics Europe; 2023. [cited 2026 Oct 8] Available from: https://plasticseurope.org/knowledge-hub/plastics-the-fast-facts-2023/.

[3] Andrady AL. Microplastics in the marine environment. Marine Pollution Bulletin 2011; 62(8): 1596-1605. https://doi.org/10.1016/j.marpolbul.2011.05.030

[4] Lavoie JA, Boulay A, Bulle C. Aquatic micro- and nano-plastics in life cycle assessment: Development of an effect factor for the quantification of their physical impact on biota. Journal of Industrial Ecology 2022; 26(6): 2123-2135. https://doi.org/10.1111/jiec.13140

[5] Barnes DKA, Galgani F, Thompson RC, Barlaz M. Accumulation and fragmentation of plastic debris in global environments. Philosophical Transactions of the Royal Society B-Biological Sciences 2009; 364(1526): 1985-1998. https://doi.org/10.1098/rstb.2008.0205

[6] Carpenter EJ, Smith KL Jr. Plastics on the Sargasso Sea Surface. Science 1972; 175(4027): 1240-1241. https://doi.org/10.1126/science.175.4027.1240

[7] Thompson RC, Olsen Y, Mitchell RP, Davis A, Rowland SJ, John AWG, McGonigle D, Russell AE. Lost at Sea: Where Is All the Plastic? Science 2004; 304(5672): 838-838. https://doi.org/10.1126/science.1094559

[8] de Souza Machado AA, Kloas W, Zarfl C, Hempel S, Rillig MC. Microplastics as an emerging threat to terrestrial ecosystems. Global Change Biology 2018; 24(4): 1405-1416. https://doi.org/10.1111/gcb.14020

[9] Xu S, Ma J, Ji R, Pan K, Miao AJ. Microplastics in aquatic environments: Occurrence, accumulation, and biological effects. Science of The Total Environment 2020; 703: 134699. https://doi.org/10.1016/j.scitotenv.2019.134699

[10] Zhao M, Cao Y, Chen T, Li H, Tong Y, Fan W, Xie Y, Tao Y, Zhou J. Characteristics and source-pathway of microplastics in freshwater system of China: A review. Chemosphere 2022; 297: 134192. https://doi.org/10.1016/j.chemosphere.2022.134192

[11] Lebreton LCM, van der Zwet J, Damsteeg JW, Slat B, Andrady A, Reisser J. River plastic emissions to the world's oceans. Nature Communications 2017; 8(1): 15611. https://doi.org/10.1038/ncomms15611

[12] Wagner M, Scherer C, Alvarez-Muñoz D, Brennholt N, Bourrain X, Buchinger S, Fries E, Grosbois C, Klasmeier J, Marti T, Rodriguez-Mozaz S, Urbatzka R, Vethaak AD, Winther-Nielsen M, Reifferscheid G. Microplastics in freshwater ecosystems: what we know and what we need to know. Environmental Sciences Europe 2014; 26(1): 12. https://doi.org/10.1186/s12302-014-0012-7

[13] Yao MX, Bai X, Xu ZJ, Li FJ, Lu Y, Li C, Hua ZL. Distribution, sources, and storage of microplastics in surface sediments of Luoma Lake. Environmental Science 2022; 43(5): 2566-2574. https://doi.org/10.13227/j.hjkx.202108270

[14] Cole M, Lindeque P, Halsband C, Galloway TS. Microplastics as contaminants in the marine environment: A review. Marine Pollution Bulletin 2011; 62(12): 2588-2597. https://doi.org/10.1016/j.marpolbul.2011.09.025

[15] Jiang C, Yin L, Li Z, Wen X, Luo X, Hu S, Yang H, Long Y, Deng B, Huang L, Liu Y. Microplastic pollution in the rivers of the Tibet Plateau. Environmental Pollution 2019; 249: 91-98. https://doi.org/10.1016/j.envpol.2019.03.022

[16] Zettler ER, Mincer TJ, Amaral-Zettler LA. Life in the "Plastisphere": Microbial Communities on Plastic Marine Debris. Environmental Science & Technology 2013; 47(13): 7137-7146. https://doi.org/10.1021/es401288x

[17] Amaral-Zettler LA, Zettler ER, Mincer TJ. Ecology of the plastisphere. Nature Reviews Microbiology 2020; 18(3): 139-151. https://doi.org/10.1038/s41579-019-0308-0

[18] Sørensen L, Rogers E, Altin D, Salaberria I, Booth AM. Sorption of PAHs to microplastic and their bioavailability and toxicity to marine copepods under co-exposure conditions. Environmental Pollution 2020; 258: 113844. https://doi.org/10.1016/j.envpol.2019.113844

[19] Tulloch CL, Cotterell BM, Pântea I, Jones DL, Golyshin PN. Selective microbial attachment to LDPE plastic beads during passage through the wastewater network. Chemosphere 2024; 362: 142618. https://doi.org/10.1016/j.chemosphere.2024.142618

[20] Niu L, Li Y, Li Y, Hu Q, Wang C, Hu J, Zhang W, Wang L, Zhang C, Zhang H. New insights into the vertical distribution and microbial degradation of microplastics in urban river sediments. Water Research 2021; 188: 116449. https://doi.org/10.1016/j.watres.2020.116449

[21] Song X, Zou H, Zhang Y, Yang J, Ding J. Microplastics alter the microbiota-mediated phosphorus profiles at sediment-water interface: Distinct microbial effects between sediment and plastisphere. Science of The Total Environment 2024; 933: 173048. https://doi.org/10.1016/j.scitotenv.2024.173048

[22] Kettner MT, Rojas-Jimenez K, Oberbeckmann S, Labrenz M, Grossart HP. Microplastics alter composition of fungal communities in aquatic ecosystems. Environmental Microbiology 2017; 19(11): 4447-4459. https://doi.org/10.1111/1462-2920.13891

[23] Nguyen HT, Choi W, Kim EJ, Cho K. Microbial community niches on microplastics and prioritized environmental factors under various urban riverine conditions. Science of The Total Environment 2022; 849: 157781. https://doi.org/10.1016/j.scitotenv.2022.157781

[24] Chigwada AD, Kalu CM, Tekere M. Substrate-specific bacterial and fungal communities in the Jukskei River plastisphere revealed by full-length amplicon sequencing. Science of The Total Environment 2026; 1042: 181894. https://doi.org/10.1016/j.scitotenv.2026.181894

[25] Prata JC, da Costa JP, Duarte AC, Rocha-Santos T. Methods for sampling and detection of microplastics in water and sediment: A critical review. TrAC Trends in Analytical Chemistry 2019; 110: 150-159. https://doi.org/10.1016/j.trac.2018.10.029

[26] Huang Z, Hu B, Wang H. Analytical methods for microplastics in the environment: a review. Environmental Chemistry Letters 2023; 21(1): 383-401. https://doi.org/10.1007/s10311-022-01525-7

[27] Hidalgo-Ruz V, Gutow L, Thompson RC, Thiel M. Microplastics in the marine environment: A review of the methods used for identification and quantification. Environmental Science & Technology 2012; 46(6): 3060-3075. https://doi.org/10.1021/es2031505

[28] Käppler A, Fischer D, Oberbeckmann S, Schernewski G, Labrenz M, Eichhorn KJ, Voit B. Analysis of environmental microplastics by vibrational microspectroscopy: FTIR, Raman or both? Analytical and Bioanalytical Chemistry 2016; 408(29): 8377-8391. https://doi.org/10.1007/s00216-016-9956-3

[29] International Organization for Standardization. Principles for the analysis of microplastics present in the environment. ISO 24187:2023. Geneva, Switzerland: International Organization for Standardization; 2023. [cited 2026 Oct 8] Available from: https://www.iso.org/standard/78033.html.

[30] Chen S, Zhou Y, Chen Y, Gu J. fastp: an ultra-fast all-in-one FASTQ preprocessor. Bioinformatics 2018; 34(17): i884-i890. https://doi.org/10.1093/bioinformatics/bty560

[31] Li YF, Xia YQ, Li XB, Xiong ZQ, Yan XY. Spatiotemporal variation of total nitrogen and total phosphorus in typical sections of the Qinhuai River. Environmental Science 2013; 34(1): 91-97. https://doi.org/10.13227/j.hjkx.2013.01.024

[32] Schloss PD, Westcott SL, Ryabin T, Hall JR, Hartmann M, Hollister EB, Lesniewski RA, Oakley BB, Parks DH, Robinson CJ, Sahl JW, Stres B, Thallinger GG, Van Horn DJ, Weber CF. Introducing mothur: open-source, platform-independent, community-supported software for describing and comparing microbial communities. Applied and Environmental Microbiology 2009; 75(23): 7537-7541. https://doi.org/10.1128/AEM.01541-09

[33] Segata N, Izard J, Waldron L, Gevers D, Miropolsky L, Garrett WS, Huttenhower C. Metagenomic biomarker discovery and explanation. Genome Biology 2011; 12(6): R60. https://doi.org/10.1186/gb-2011-12-6-r60

[34] Zhang SJ, Zeng YH, Zhu JM, Cai ZH, Zhou J. The structure and assembly mechanisms of plastisphere microbial community in natural marine environment. Journal of Hazardous Materials 2022; 421: 126780. https://doi.org/10.1016/j.jhazmat.2021.126780

[35] McCormick A, Hoellein TJ, Mason SA, Schluep J, Kelly JJ. Microplastic is an abundant and distinct microbial habitat in an urban river. Environmental Science & Technology 2014; 48(20): 11863-11871. https://doi.org/10.1021/es503610r

[36] Burgaud G, Henry N, Corre E, Pujo-Pay M, Conan P, Hingant M, Meistertzheim AL, Barbe V, Paul-Pont I, ter Halle A, Eyheraguibel B, Ludwig W, Kedzierski M, Briand JF, Siano R, Meyneng M, Lepère C, Ghiglione JF. A comprehensive pan-European exploration of fungal plastisphere dynamics along river-to-sea continuums. Journal of Hazardous Materials 2026; 514: 142613. https://doi.org/10.1016/j.jhazmat.2026.142613

[37] Hurley R, Woodward J, Rothwell JJ. Microplastic contamination of river beds significantly reduced by catchment-wide flooding. Nature Geoscience 2018; 11(4): 251-257. https://doi.org/10.1038/s41561-018-0080-1

[38] Miao L, Yu Y, Adyel TM, Wang C, Liu Z, Liu S, Huang L, You G, Meng M, Qu H, Hou J. Distinct microbial metabolic activities of biofilms colonizing microplastics in three freshwater ecosystems. Journal of Hazardous Materials 2021; 403: 123577. https://doi.org/10.1016/j.jhazmat.2020.123577

[39] Seeley ME, Song B, Passie R, Hale RC. Microplastics affect sedimentary microbial communities and nitrogen cycling. Nature Communications 2020; 11(1): 2372. https://doi.org/10.1038/s41467-020-16235-3

[40] Niu L, Chen Y, Li Y, Wang Y, Shen J, Wang L, Zhang W, Zhang H, Zhao B. Diversity, abundance and distribution characteristics of potential polyethylene and polypropylene microplastic degradation bacterial communities in the urban river. Water Research 2023; 232: 119704. https://doi.org/10.1016/j.watres.2023.119704

https://doi.org/10.12974/2311-8741.2026.14.08

© 2026 Chen *et al.*
This is an open-access article licensed under the terms of the Creative Commons Attribution License (http://creativecommons.org/licenses/by/4.0/), which permits unrestriced use, distribution, and reproduction in any medium, provided the work is properly cited.